

One-dimensional ferromagnetic classical-spin-field model*

A. R. McGurn and D. J. Scalapino

Department of Physics, University of California, Santa Barbara, California 93106

(Received 4 September 1974)

A continuum generalization of a one-dimensional classical ferromagnetic Heisenberg exchange-coupled spin model is solved. The field-dependent susceptibilities, specific heat, and correlation lengths are determined. The zero-field susceptibilities and correlation lengths in the presence of single-ion anisotropy energy are also calculated. The field-dependent properties are determined for the case in which the field is parallel to the single-ion anisotropy axis, and the anisotropy energy is positive. The model approximates the low-temperature behavior of the discrete spin system in the region in which spins become correlated over distances large compared to a lattice constant.

I. INTRODUCTION

There are a number of magnetic materials in which the molecular geometry is such that the exchange coupling between spins along certain one-dimensional chains is much larger than the coupling between the chains.^{1,2} Above a three-dimensional ordering temperature determined by the interchain coupling, these systems can be described in terms of one-dimensional models.^{3,4} Another consequence of the geometry of these pseudo-one-dimensional systems is that the exchange coupling along a chain, although it is much larger than the interchain coupling, is often sufficiently weak that the Zeeman energy can be made comparable with it. This circumstance makes it possible to investigate the non-linear magnetic-field dependence of the magnetization, specific heat, and correlation lengths. A particularly interesting region to study this field dependence is that in which the temperature is sufficiently low that there are well developed short-range spin correlations due to the exchange coupling.

Here we propose to treat the low-temperature field-dependent properties of such one-dimensional ferromagnetic exchange-coupled systems¹ in terms of a classical-spin-field model.⁵ This model is a continuum approximation of the classical Heisenberg model discussed by Fisher.³ Mathematically it represents a limit in which both the spin and the correlation length become infinite. Physically, it provides a useful description when $S > \frac{1}{2}$ and when the correlations of the spins extend over several lattice spacings. Moreover, the statistical mechanics of the spin-field model in an external magnetic field can be calculated using the same functional integral techniques which have been applied to the Ginzburg-Landau field.⁶ In this approach, the classical statistical mechanics problem is reduced to the problem of calculating the first few eigenvalues and eigenvectors of an effective Hamiltonian.

In Sec. II, the spin-field Hamiltonian is obtained as the continuum limit of a classical discrete spin

system. The interactions include an isotropic exchange coupling, a single-ion anisotropy energy, and the Zeeman coupling to an external magnetic field. Using this spin-field Hamiltonian, the various physical quantities of interest are expressed in terms of functional integrals over the spin field. The evaluation of these functional integrals is then shown to be equivalent to the solution of the quantum-mechanical problem of a hindered rotor.

In subsection A of Sec. III, numerical solutions are obtained for the case in which the single-ion anisotropy energy vanishes. Results for the field dependence of the magnetization, susceptibility, specific heat, and spin-spin correlation functions are given. It is possible to plot a number of these results in terms of the single dimensionless variable $kT/\sqrt{2Jg\mu H}$, where J is the exchange coupling, and $g\mu H$ is the Zeeman energy.

The effect of the single-ion anisotropy interaction is discussed in subsection B of Sec. III. Results for the zero-field spin-spin correlation functions and susceptibilities are given. The field and temperature dependence of the magnetization and correlation length for the case in which the external field is parallel to the anisotropy axis are discussed. A summary and conclusion is given in Sec. IV.

II. THEORY

The functional integration techniques developed in the study of the one-dimensional Ginzburg-Landau problem⁶ are applied to calculate the statistical mechanics of a one-dimensional classical spin field in an external magnetic field. We are specifically interested in the low-temperature properties where the spin field is slowly varying over a distance of many lattice spacings.

For a system of discrete exchange coupled classical spins the Hamiltonian is

$$\mathcal{H}_0 = -\sum_i 2J\vec{S}_i \cdot \vec{S}_{i+1} - g\mu H \sum_i S_{zi} + D \sum_i (S_{zi})^2. \quad (1)$$

Here \vec{S}_i are classical spins of unit magnitude occupying discrete lattice sites and $J > 0$ (ferromag-

netic coupling). The second term represents the Zeeman energy, and the last term is the single-ion anisotropy. For $D > 0$, the external field points along the hard axis of magnetization. The exchange term in Eq. (1) can be written, to within a constant, as

$$\sum_i a(Ja) \left| \frac{\vec{S}_{i+1} - \vec{S}_i}{a} \right|^2, \quad (2)$$

with a the lattice spacing. If \vec{S}_i is a slowly varying function of the site index, we can approximate the discrete spin problem by the continuum limit.⁷ In this case $|\vec{S}_{i+1} - \vec{S}_i|/a$ can be replaced by $|d\vec{S}/dx|$ and Eq. (1) becomes

$$\mathcal{H}_0[\vec{S}(x)] = \int dx \left(J \left| \frac{d\vec{S}(x)}{dx} \right|^2 - h S_z(x) + D [S_z(x)]^2 \right). \quad (3)$$

Here we measure lengths in units of the lattice spacing a and set $h = g\mu H$. Furthermore, $\vec{S}(x) = \hat{n}(x)$, where $\hat{n}(x)$ is a unit vector at point x .

Now the statistical mechanics can be expressed formally in terms of functional integrals over the continuous vector field $\vec{S}(x)$. The partition function is given by

$$Z = \int \delta\vec{S}(x) e^{-\beta \mathcal{H}_0[\vec{S}(x)]} \quad (4)$$

and the expectation values of physical quantities such as $S_z(x)$ is

$$\langle S_z(x) \rangle = \int \delta\vec{S}(x) \frac{e^{-\beta \mathcal{H}_0[\vec{S}(x)]}}{Z} S_z(x). \quad (5)$$

In addition we will be interested in the correlation functions

$$g_{zz}(x) = \langle S_z(x) S_z(0) \rangle - \langle S_z^2 \rangle \quad (6)$$

and

$$g_{xx}(x) = \langle S_x(x) S_x(0) \rangle, \quad (7)$$

where by symmetry $g_{xx}(x) = g_{yy}(x)$. Here

$$\langle S_i(x) S_i(0) \rangle = \int \delta\vec{S}(x) S_i(x) S_i(0) \frac{e^{-\beta \mathcal{H}_0[\vec{S}(x)]}}{Z}. \quad (8)$$

These functional integrals over one-dimensional fields can be evaluated by transfer matrix techniques. In the usual way,⁶ this reduces the computational problem to finding the eigenstates and eigenvalues of an effective Hamiltonian

$$\mathcal{H}|n\rangle = \left(\frac{\vec{\mathcal{L}}^2}{4\beta^2 J} - h \cos\theta + D \cos^2\theta \right) |n\rangle = E_n |n\rangle. \quad (9)$$

Here $\vec{\mathcal{L}}$ is the angular momentum so that

$$\vec{\mathcal{L}}^2 = -\frac{1}{\sin\theta} \frac{\partial}{\partial\theta} \sin\theta \frac{\partial}{\partial\theta} - \frac{1}{\sin^2\theta} \frac{\partial^2}{\partial\varphi^2}, \quad (10)$$

and \mathcal{H} describes a quantum-mechanical hindered rotor. For a chain with periodic boundary conditions the partition function, Eq. (4), is equal to

$$Z = e^{-\beta \Delta E L} \sum_n e^{-\beta E_n L} \quad (11)$$

with

$$\Delta E = kT \ln(\beta 2J_{c1}) - 2J_{c1}. \quad (12)$$

In the limit where the length of the chain L is large compared to the spin-spin correlation length, the lowest eigenvalue determines Z and

$$Z \cong e^{-\beta(\Delta E + E_0)L}, \quad (13)$$

the free energy per unit length is therefore simply $\Delta E + E_0$.

The expectation values of $S_i(x)$ involve matrix elements of $S_x = \cos\theta$, $S_y = \sin\theta \cos\varphi$ and $S_z = \sin\theta \sin\varphi$. Again for L large compared to the spin-spin correlation length the results simplify and, for example, $\langle S_z \rangle$ is equal to the ground-state matrix element of $\cos\theta$

$$\langle S_z \rangle = \langle 0 | \cos\theta | 0 \rangle. \quad (14)$$

Alternatively the magnetization per site normalized by $g\mu$ is equal to $\langle S_z \rangle$. Since the magnetic-field dependent part of the free energy per spin is E_0 ,

$$\langle S_z \rangle = -\frac{1}{g\mu} \frac{\partial}{\partial H} E_0 = -\frac{\partial E_0}{\partial h}. \quad (15)$$

The S_x - S_x correlation function is given by

$$g_{xx}(x) = \sum_{n \neq 0} |\langle n | \cos\theta | 0 \rangle|^2 e^{-\beta x(E_n - E_0)}. \quad (16)$$

Because \mathcal{H} is invariant under rotations about the z axis, the excited states $|n\rangle$ in Eq. (16) have magnetic quantum number $m = 0$. The large x dependence of Eq. (16) is set by the lowest eigenvalue E_1 and a good approximation to Eq. (16) is simply

$$g_{xx}(x) \cong |\langle 1 | \cos\theta | 0 \rangle|^2 e^{-x/\xi_{xx}}. \quad (17)$$

Here the correlation length ξ_{xx} is given by

$$\xi_{xx}^{-1} = \beta(E_1 - E_0). \quad (18)$$

In the same approximation, the g_{xx} correlation is

$$g_{xx}(x) \cong 2 |\langle 1' | \sin\theta \cos\varphi | 0 \rangle|^2 e^{-x/\xi_{xx}}, \quad (19)$$

with

$$\xi_{xx}^{-1} = \beta(E_{1'} - E_0). \quad (20)$$

The eigenvalue $E_{1'}$ is that of the lowest eigenstate $|1'\rangle$ with $m = \pm 1$ and the factor of 2 in Eq. (19) comes from the twofold degeneracy of this level.

The susceptibilities of the spin field can be expressed in terms of the correlation functions,

$$\chi_{ii} = \frac{g^2 \mu^2}{kT} \int g_{ii}(x) dx, \quad (21)$$

where the integral is over the one-dimensional lattice. From Eqs. (16) and (19) it follows that

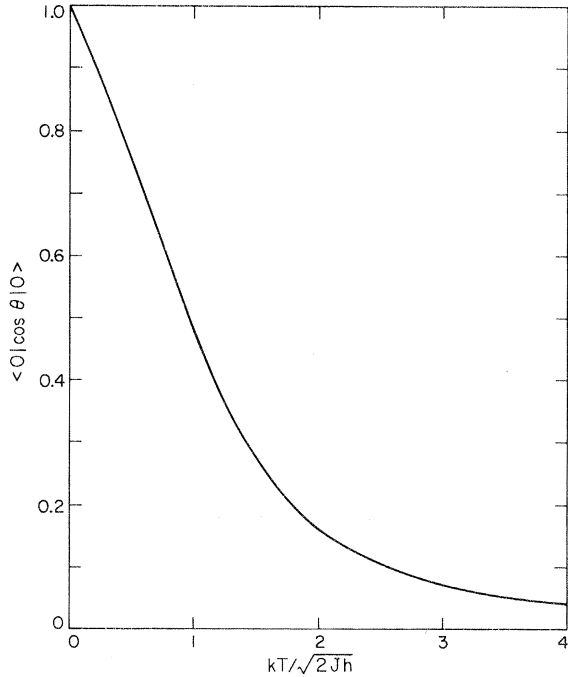


FIG. 1. Plot of $\langle S_z \rangle = \langle 0 | \cos \theta | 0 \rangle$ vs $kT/\sqrt{2J\hbar}$ with $D=0$ and $h \neq 0$.

$$\chi_{zz} = \frac{g^2 \mu^2}{kT} 2 \sum_n [\beta(E_n - E_0)]^{-1} |\langle n | \cos \theta | 0 \rangle|^2$$

$$\approx \frac{g^2 \mu^2}{kT} 2 \xi_{zz} |\langle 1 | \cos \theta | 0 \rangle|^2, \quad (22)$$

and

$$\chi_{xx} = \frac{g^2 \mu^2}{kT} 4 \xi_{xx} |\langle 1' | \sin \theta \cos \varphi | 0 \rangle|^2. \quad (23)$$

III. CALCULATIONS

In order to evaluate the quantities discussed in the previous section we must calculate the ground-state and low-lying-excited-state eigenvalues and eigenfunctions of Eq. (9). This is readily accomplished by constructing a matrix representation of \mathcal{H} in a basis of spherical harmonics and numerically diagonalizing it. The rotational invariance of \mathcal{H} about the z axis leads to a block-diagonal form for \mathcal{H} in which Y_{lm} states with different m values form separate blocks. The ground state E_0 is in the manifold $m=0$ as well as the excited state E_1 . The only additional manifold which we will consider is the $m=1$ manifold whose lowest energy state is $E_{1'}$. Adequate convergence was obtained using 25×25 matrices.

A. Zero single-ion anisotropy ($D=0$)

First we consider the case in which the single-ion anisotropy energy can be neglected. Setting D

$= 0$ in Eq. (9), it follows that the eigenvalues E_n of \mathcal{H} can be written as

$$\beta^2 J E_n = \epsilon_n(\beta^2 J \hbar). \quad (24)$$

Here ϵ_n does not depend separately upon β , $2J$, and \hbar but only upon the dimensionless combination $\beta^2 J \hbar$. The magnetization per spin (normalized to $g\mu$) is just $\langle S_z \rangle$ which can be obtained by differentiating E_0 with respect to \hbar [see Eq. (15)],

$$\langle S_z \rangle = -\frac{\partial}{\partial \hbar} E_0 = -\epsilon'_0(\beta^2 J \hbar). \quad (25)$$

Thus when $D=0$, $\langle S_z \rangle$ depends only upon the variable $\beta^2 J \hbar$. In presenting our results, we have chosen to use the reduced temperature $kT/\sqrt{2J\hbar} = (2\beta^2 J \hbar)^{-1/2}$. In Fig. 1, $\langle S_z \rangle$ is plotted versus this reduced temperature. It attains its zero-temperature value linearly as $kT/\sqrt{2J\hbar}$ goes to zero.

In the absence of a magnetic field the spin-spin correlation length is determined by the eigenvalues of $\mathcal{L}^2/4\beta^2 J$: $l(l+1)/4\beta^2 J$ with $l=0, 1, \dots$

$$\xi = kT(E_1 - E_0)^{-1} = \frac{2J}{kT}. \quad (26)$$

Thus for $h=0$, we obtain the well-known result that ξ diverges as T^{-1} for $kT \ll J$. In the presence of an external field, the quantities $\xi_{zz}\sqrt{\hbar/2J}$ and $\xi_{xx}\sqrt{\hbar/2J}$ depend only upon the reduced temperature $kT/\sqrt{2J\hbar}$. Plots of $\xi_{zz}\sqrt{\hbar/2J}$ and $\xi_{xx}\sqrt{\hbar/2J}$ versus the reduced temperature are shown in Fig. 2. At reduced temperatures greater than unity, the correlation lengths approach the field-independent result of Eq. (26). For $kT/\sqrt{2J\hbar}$ less than unity the correlation lengths saturate. In order to see more clearly how the spin-spin correlations are modified by an external field, we have plotted ξ_{zz} and ξ_{xx} versus kT/J for various h/J ratios in Figs. 3 and 4, respectively. As the temperature is lowered ξ_{zz} drops below its

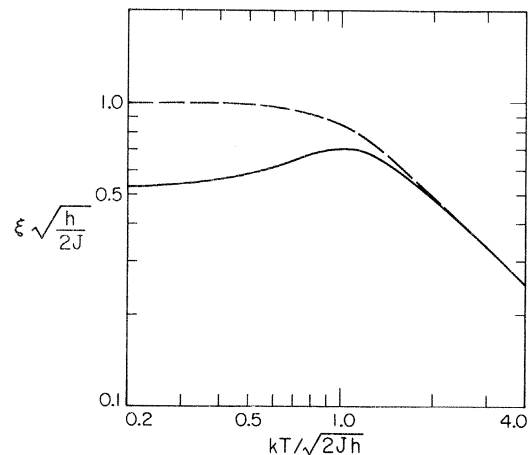


FIG. 2. Plot of $\xi_{zz}\sqrt{\hbar/2J}$ (solid line) and $\xi_{xx}\sqrt{\hbar/2J}$ (dashed line) vs $kT/\sqrt{2J\hbar}$ for $D=0$ and $h \neq 0$.

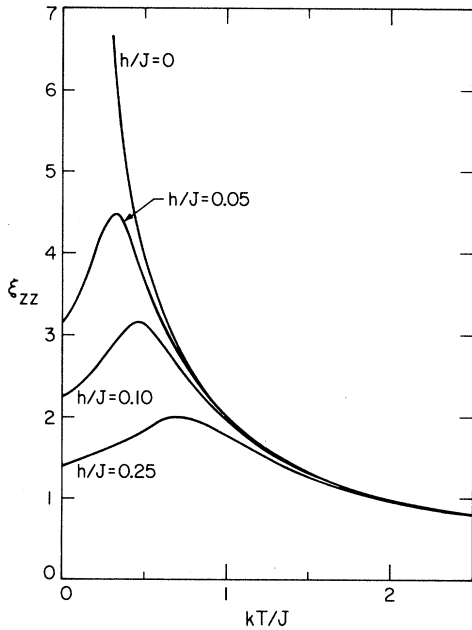


FIG. 3. Plot of ξ_{zz} vs kT/J for various h/J ratios with $D=0$ and $h \neq 0$.

$h=0$ value and through a maximum. This maximum occurs when $h\xi \sim kT$ and corresponds to the point at which the Zeeman energy of a group of spins correlated over $\xi \sim 2J/kT$ becomes equal to kT . At still lower temperatures the spins are sufficiently polarized by the external field that ξ_{zz} should be viewed as a healing length. This healing length for

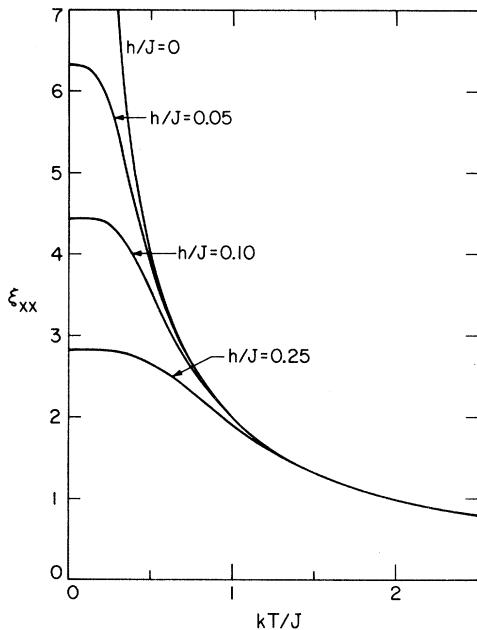


FIG. 4. Plot of ξ_{xx} vs kT/J for various h/J ratios with $D=0$ and $h \neq 0$.

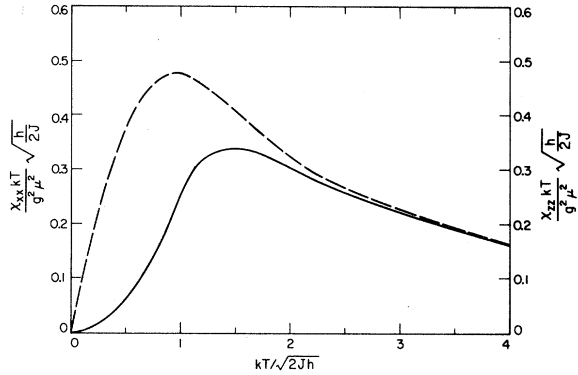


FIG. 5. Plot of $(\chi_{zz}/g^2\mu^2)kT\sqrt{h/2J}$ (solid line) and $(\chi_{xx}/g^2\mu^2)kT\sqrt{h/2J}$ (dashed line) vs $kT/\sqrt{2Jh}$ for $D=0$ and $h \neq 0$.

a disturbance of the spins from the polarized state decreases as the thermal disruption associated with kT goes to zero. The saturation of ξ_{xx} at low temperatures shown in Fig. 4 is a reflection of the ordering of the spins along H .

In Fig. 5, the parallel and perpendicular field-dependent susceptibilities per spin are plotted versus the reduced temperature. Note that χ_{zz} and χ_{xx} for each temperature are decreased from their zero-field values which diverge as $1/T^2$ at low temperatures. This is further evidence of the suppression of spin fluctuations due to the external field alignment. In the presence of a field, χ_{zz} goes to zero linearly as T vanishes and χ_{xx} approaches a constant.

The free energy per unit length (or per spin) E_0 gives the change in free energy due to the presence of the external field. Calculating the specific heat associated with E_0 leads to the change ΔC in specific heat per spin due to the magnetic field

$$\Delta C = -T \frac{\partial^2}{\partial T^2} E_0 \quad (27)$$

This change in specific heat per spin in units of k multiplied by the factor $\sqrt{2J/h}$ is plotted versus the reduced temperature in Fig. 6. For $kT/\sqrt{2Jh} > 2.0$,

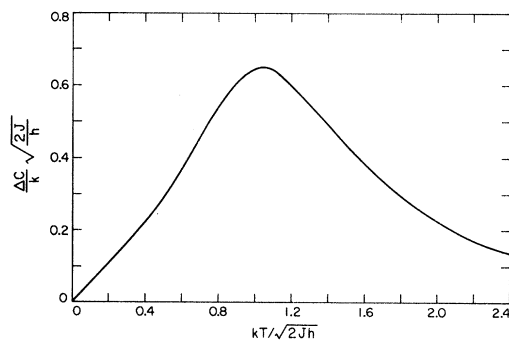


FIG. 6. Plot of $(\Delta C/k)\sqrt{2J/h}$ vs $kT/\sqrt{2Jh}$ for $D=0$ and $h \neq 0$.

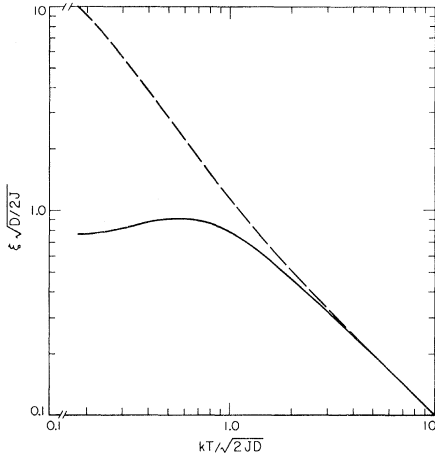


FIG. 7. Plot of $\xi_{zz}\sqrt{D/2J}$ (solid line) and $\xi_{xx}\sqrt{D/2J}$ (dashed line) vs $kT/\sqrt{2J|D|}$ for $H=0$ and $D>0$.

$\Delta C\sqrt{2J}/k\sqrt{h}$ varies as $2(2Jh)^{3/2}/(kT)^3$. The peak in the field-dependent specific heat occurs when $kT \cong 2Jh/kT$.

B. Nonvanishing single-ion anisotropy ($D \neq 0$)

In this part, results for the zero-field ($h=0$) correlation functions and susceptibilities in the presence of single-ion anisotropy ($D \neq 0$) are discussed. Also, the order parameter $\langle S_z \rangle$ and the correlation lengths for an external magnetic field parallel to the axis of the single ion anisotropy are calculated for $D>0$. For $h=0$, it follows from the Hamiltonian, Eq. (9), that

$$\beta^2 J E_n = \tilde{\epsilon}_n(\beta^2 J D). \quad (28)$$

Thus the appropriate reduced temperature variable is $kT/\sqrt{2J|D|}$.

The $h=0$ correlation lengths ξ_{xx} and ξ_{zz} are plotted versus $kT/\sqrt{2J|D|}$ for $D>0$ and $D<0$ in Figs.

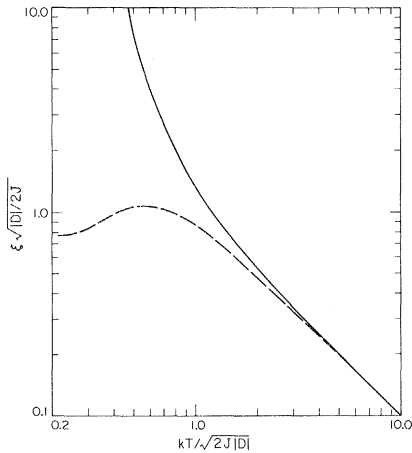


FIG. 8. Plot of $\xi_{zz}\sqrt{|D|/2J}$ (solid line) and $\xi_{xx}\sqrt{|D|/2J}$ (dashed line) vs $kT/\sqrt{2J|D|}$ for $H=0$ and $D<0$.

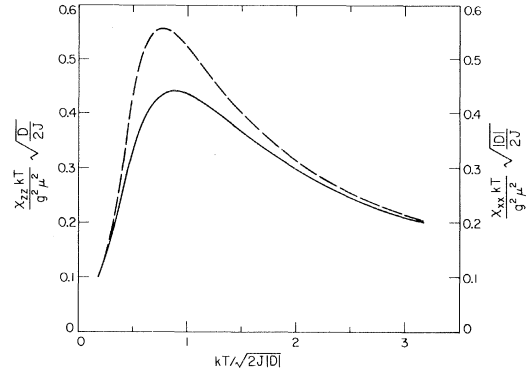


FIG. 9. Plot of $(\chi_{zz}kT/g^2\mu^2)\sqrt{D/2J}$ for $D>0$ (solid line) and $(\chi_{xx}kT/g^2\mu^2)\sqrt{|D|/2J}$ for $D<0$ (dashed line) vs $kT/\sqrt{2J|D|}$ for $h=0$.

7 and 8, respectively. For $D>0$, ξ_{xx} is greater than ξ_{zz} and as the temperatures go to zero ξ_{xx} diverges whereas ξ_{zz} approaches a constant value. For $D<0$, ξ_{xx} is always less than ξ_{zz} and at low temperatures ξ_{xx} approaches a constant while ξ_{zz} diverges. The peaks of ξ_{zz} for $D>0$ and ξ_{xx} for $D<0$ occur when the anisotropy energy of the spins contained in a coherence length $\xi \sim 2J/kT$ is of order kT (i. e., $D\xi = 2JD/kT \cong kT$). At lower temperatures, the anisotropy produces a crossover from Heisenberg- to Ising-like behavior for $D<0$ and planar x - y behavior for $D>0$. This reduction of the rotational symmetry is responsible for the rapid growth of ξ_{zz} for $D<0$ and ξ_{xx} for $D>0$.

The zero-field susceptibilities χ_{xx} for $D<0$ and χ_{zz} for $D>0$ are plotted versus the reduced temperature $kT/\sqrt{2J|D|}$ in Fig. 9. This corresponds to the magnetic susceptibility in the hard direction. The susceptibilities for the easy axis χ_{zz} for $D<0$ and easy plane χ_{xx} for $D>0$ are shown in Fig. 10.

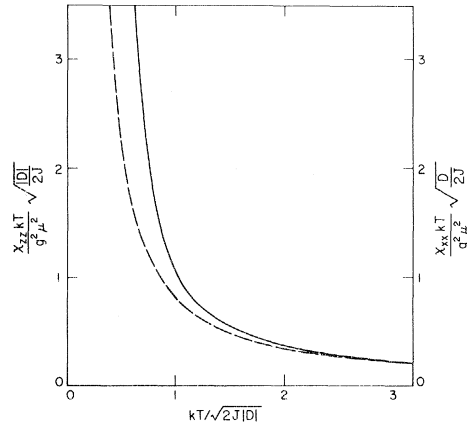


FIG. 10. Plot of $(\chi_{zz}kT/g^2\mu^2)\sqrt{|D|/2J}$ for $D<0$ (solid line) and $(\chi_{xx}kT/g^2\mu^2)\sqrt{D/2J}$ for $D>0$ (dashed line) vs $kT/\sqrt{2J|D|}$ for $h=0$.

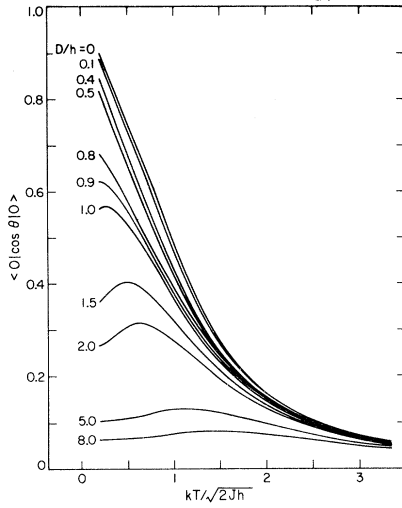


FIG. 11. Plot of $\langle S_z \rangle = \langle 0 | \cos \theta | 0 \rangle$ vs $kT/\sqrt{2J\hbar}$ for various ratios of $D/h > 0$.

These figures indicate that the zero-field susceptibility and correlation functions are greater in the directions in which the anisotropy energy most favors spin alignment.

We conclude by discussing some results obtained when a magnetic field is applied parallel to the anisotropy axis and D is positive. The magnetization per site normalized to $g\mu$ is equal to $\langle 0 | \cos \theta | 0 \rangle$ which is plotted versus $kT/\sqrt{2J\hbar}$ for various D/h ratios in Fig. 11. As D increases, spin alignment along the z direction is suppressed and the magnetization is reduced. For $D/h > 1$ a peak in the magnetization versus $kT/\sqrt{2J\hbar}$ appears. Fig. 12 shows the behavior of the ξ_{zz} correlation length for increasing ratios of the anisotropy to Zeeman energy. Consider a fixed value of the reduced temperature $kT/\sqrt{2J\hbar}$ less than unity. As D increases from zero, the ξ_{zz} correlation length at first increases, then passes through a maximum for $D \approx \hbar$. As D increases beyond \hbar , ξ_{zz} decreases.

IV. CONCLUSIONS

We have calculated the low-temperature properties of a one-dimensional ferromagnetic spin-field model in the presence of various combinations of external magnetic field and single-crystal anisotropy terms. The spin field provides a useful approximation of the behavior of a one-dimensional chain of classical spins when the correlations extend over several lattice spacings,

$$\xi = 2J/kT > 1. \quad (29)$$

For example, in the absence of an external magnetic field and zero anisotropy, Fisher³ has shown that

$$\chi = \frac{(g\mu)^2}{3kT} \frac{1+u(\xi)}{1-u(\xi)}, \quad (30)$$

where $u(\xi) = \coth \xi - 1/\xi$ with $\xi = 2J/kT$. Expanding this for ξ large gives

$$\chi \cong \frac{(g\mu)^2}{kT} \frac{2}{3} \xi, \quad (31)$$

which is the continuum spin-field result for χ .

In addition to the requirement that $kT < 2J$, T must be larger than the critical temperature T_c associated with interchain ordering in order that a one-dimensional description be applicable. The critical temperature T_c can be estimated⁸ in terms of the interchain coupling J_{\perp} and the number of interchain near neighbors z_{\perp}

$$kT_c \sim J \sqrt{\frac{8}{3} \frac{z_{\perp} |J_{\perp}|}{J}}. \quad (32)$$

Therefore, when $z_{\perp} |J_{\perp}|/J \ll 1$ there is a range of temperatures

$$2J > kT > J \sqrt{\frac{8}{3} \frac{z_{\perp} |J_{\perp}|}{J}}, \quad (33)$$

where a continuum spin-field approximation is applicable.

We consider that one of the most important properties of the spin-field model is the facility with which one can handle various types of interactions of exchange coupled spins to obtain at least a qualitative indication of the low-temperature behavior of these types of systems. The spin-field model has been used to fit the low-temperature magnetic properties of the one-dimensional ferromagnetic material CsNiF_3 .⁵ Unfortunately our theory, as presently developed, does not adequately treat the antiferromagnet in an external field to yield significant corrections. But the zero-field properties of the antiferromagnet in the presence of a single-ion anisotropy term have been calculated.⁹

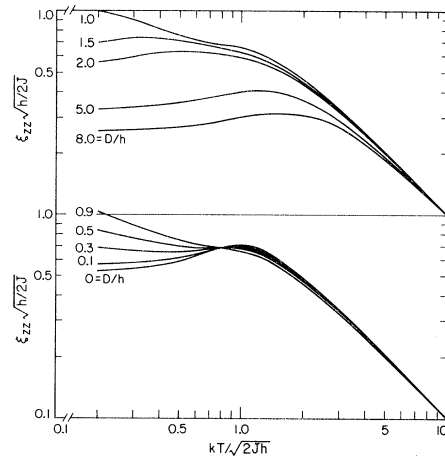


FIG. 12. Plot of $\xi_{zz} \sqrt{\hbar/2J}$ vs $kT/\sqrt{2J\hbar}$ for various ratios of $D/h > 0$.

*Research supported by the National Science Foundation.

¹M. Steiner, W. Krieger, and O. Babel, *Solid State Commun.* 9, 227 (1971); M. Steiner and B. Dorner, *Solid State Commun.* 12, 537 (1973).

²M. T. Hutchings, G. Shirane, R. J. Birgeneau, and S. L. Holt, *Phys. Rev. B* 5, 1999 (1972).

³M. Fisher, *Am. J. Phys.* 32, 343 (1964).

⁴E. H. Lieb and D. C. Mattis, *Mathematical Physics in One Dimension* (Academic, New York, 1966).

⁵A. R. McGurn, P. A. Montano, and D. J. Scalapino, *Solid State Commun.* (to be published).

⁶D. J. Scalapino, M. Sears, and R. A. Ferrell, *Phys. Rev. B* 6, 3409 (1972).

⁷C. Herring and C. Kittel, *Phys. Rev.* 81, 869 (1951).

⁸D. J. Scalapino, Y. Imry, and P. Pincus (unpublished).

⁹A. R. McGurn, Ph.D. thesis (University of California, Santa Barbara) (unpublished).